Enhanced photocatalytic properties of ZnO nanostructures by fine pomegranate peel powder towards photodegradation of malachite green under natural sunlight irradiation

Sahiba Mastoi[1], Atef AbdelKader[7], Muhammad Ali Bhatti[1], Aneela Tahira[3], Mushtaque Ali Jakhrani[3], Abdul Manan[1], Shusheel Kumar[4], Aqeel Ahmed Shah[8], Shyma S Medany[6], Ayman Nafady[5], Elmuez A. Dawi[7], Abd Al Karim Haj Ismail[7] and Zafar Hussain Ibupoto[2*]

[1]Centre for Environmental Sciences, University of Sindh Jamshoro, 76080, Sindh Pakistan. [2]Institute of Chemistry, University of Sindh Jamshoro, 76080, Sindh Pakistan.
[3]Institute of Chemistry, Shah Abdul Latif University Khairpur Mirs, Sindh, Pakistan.
[4]Institute of Physics, University of Sindh Jamshoro, 76080, Sindh Pakistan.
[5]Chemistry Department, College of Science, King Saud University, Riyadh, 11451, Saudi Arabia.
[6]Nanotechnology Research Centre (NTRC), The British University in Egypt (BUE), Cairo, Egypt.
[7]Nonlinear Dynamics Research Centre (NDRC), Ajman University, Ajman P.O. Box 346, United Arab Emirates.
[8]Wet Chemistry Laboratory, Department of Metallurgical Engineering, NED University of Engineering and Technology, University Road, Karachi 75270, Pakistan
*Correspondence: **author**: Zafar Hussain Ibupoto, **Email:** zaffar.ibhupoto@usindh.edu.pk

Abstract: Photocatalytic applications require efficient, earth abundant, and low cost nanostructured materials, but synthesis of these materials is a challenging undertaking. As a result of the development of green methodology, a new class of efficient surface modified nanostructured materials has been created that may be used for the photodegradation of organic dyes. Our study utilized pomegranate peel powder to synthesize ZnO nanostructures using a low temperature aqueous chemical route. Phytochemicals derived from pomegranate peel powder altered the morphology of the ZnO nanostructured material, reduced the crystallite size, decreased the optical bad gap, and resulted in zinc vacancies. Various morphology, crystal quality, chemical composition, and optical studies were carried out by scanning electron microscopy (SEM), powder X-ray diffraction (XRD), energy dispersive spectroscopy (EDS), and UV-visible spectroscopy, respectively. In the presence of natural sunlight, pomegranate peel powder greatly enhanced the photocatalytic activity of ZnO nanostructures towards the degradation of malachite green. At constant catalyst doses, ZnO photocatalyst properties were evaluated in terms of different dye concentrations, pH effects, and scavengers. A pH study revealed that almost 97.14% degradation was possible for short periods of time of 20 minutes at low concentration. During the growth process, pomegranate peel powder provided an effective source of phytochemicals, which enhanced the surface active sites and optical properties of ZnO nanostructures, leading to outstanding photodegradation for malachite green.

Keywords: Pomegranate peel powder; ZnO nanostructures; Malachite green; Photodegradation

1. Introduction

Fabric, textile, printing, and pharmaceutical industries release large quantities of wastewater into the open environment, which adversely affects the eco system, pollutes the environment, and threatens human life [1]. Organic compounds are the major constituents of dyes used in the food and textile industries, and they constitute the primary source of environmental pollution. Furthermore, these dyes possess carcinogenic properties as well as being hazardous to both human health and the environment [2]. In particular, malachite green, also known as Victoria green 4, has the chemical formula $C_{23}H_{25}N_2Cl$. The powder is greenish in color and is highly soluble in water, which is why it is widely used as a food coloring additive as well as a dye for cotton, silk, and wool [3]. Despite its low concentration, malachite green can cause mutagenic and genotoxic effects to aquatic organisms. A great deal of attention has been paid recently to the harmful effects and mitigation measures associated with malachite green for the purpose of highlighting the negative impacts on biological systems and aquatic ecosystems [4]. As a result, different technologies have

been developed to address the challenges of wastewater treatment. However, these technologies are expensive, complex, involve a number of steps, and produce secondary pollutants during operation, which has resulted in additional challenges [5]. It is therefore necessary to develop new methods and advanced technologies in order to effectively treat wastewater at low cost, conveniently, efficiently, and by using substances that are environmentally friendly and eco-friendly. Hence, the photocatalytic degradation of organic dyes has been discovered to be a promising technology to address the challenges of wastewater and is currently being studied heavily as a result of the advancement in the field of nanotechnology through the production of wide array of functional nanostructures. In this light, semiconducting nanostructures are valuable classes of material science that have been extensively studied for wastewater treatment and solar-powered hydrogen production [6-9]. Zinc oxide (ZnO) is among these materials that has been extensively studied as a photocatalytic material, owing to its advantages in both physical and chemical stability, low toxicity, abundant availability on earth, and ease of preparation in comparison to many semiconducting materials [10-13]. Due to its high quantum efficiency, ZnO exhibits relatively better enhanced photocatalytic properties than titanium dioxide (TiO_2) for solar-driven hydrogen and the degradation of organic dyes [7]. Moreover, the intrinsic point defects in ZnO enable it to absorb and exploit a wider range of solar spectrum than TiO2, leading to efficient photocatalysis in the visible range [14]. Despite the fact that ZnO has many advantages, its performance is limited as a result of the short diffusion lengths of electrons and holes generated during light irradiation, which results in rapid electron-hole recombination, thereby reducing ZnO's photocatalytic performance [15, 16]. ZnO nanostructures have been synthesized using a wide range of preparation methods, including co-precipitation [17], sol-gel [18], pulsed laser deposition [19], sol-gel spinning coating [20] and green synthesis [21]. Co-precipitation is a synthetic method that has attracted considerable attention because of its rapid preparation of ZnO nanostructures in the presence of phytochemicals from the pants and its efficient photocatalytic activity for the photodegradation of organic dyes and wastewater treatment [22]. By using plant extracts, one can obtain large quantities of water-soluble phytochemicals for the synthesis of ZnO nanostructures, which minimizes the need for complex and toxic chemicals [23-25]. It is believed that these phytochemicals act as capping, reducing, and stabilizing agents and alter the surface and optical properties of ZnO nanostructures. The pomegranate peel (PP) contains potential bioactive compounds such as phenolic acids (hydroxycinnamic and hydroxybenzoic acids), flavonoids (anthocyanins, catechins and other complex flavonoids) and hydrolysable tannins (ellagic and gallic acids, pedunculagin, punicalin and punicalagin) [26, 27, 28]. In Scheme 1, some of the active ingredients involved in the phenomenon of pomegranate peel are described.

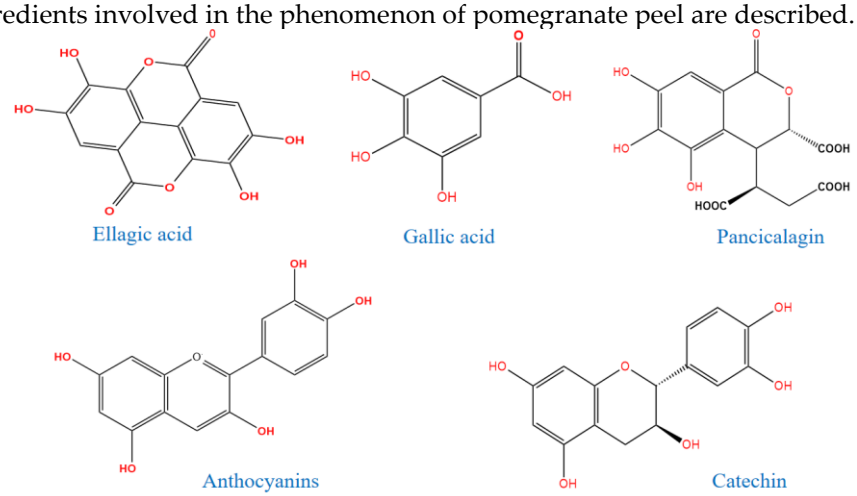

Scheme 1. Molecular structure of some of the active ingredients of phenomenon of pomegranate peel.

No existing literature has reported the photodegradation of malachite green and the effect of pomegranate peel (PP) on ZnO nanostructures. During the growth process of ZnO nanostructures, fine pomegranate peel powder was used directly, providing significant amounts of these phytochemicals which could be used to reduce, cap, and stabilize the nanostructures, thereby controlling the surface and optical properties. The optical band gap of ZnO was reduced with the use of increasing amount of pomegranate peel powder, thereby the large portion of natural sun light was exploited and efficient degradation of malachite would be expected. Moreover, the role of pomegranate peel content during the growth of ZnO through the creation of zinc vacancies and their effect on the photodegradation of synthetic dyes have not been reported yet.

Therefore, an excellent photodegradation of malachite green was demonstrated under the illumination of natural sunlight due to the decrease in the recombination rate of electron hole pairs.

2. Materials and Methods

2.1. Chemical and reagents

Zinc acetate dihydrate ($ZnC_4H_6O_4$, M=183.48), malachite green (MG) powder, ammonium hydroxide, and ethanol were obtained from Merck and were used without further purification. The peels of pomegranates were obtained from a local fruit market. Throughout the experimental activities, deionized water (DI) water was used.

2.2. Green synthesis of ZnO nanostructures using pomegranate peel powder

Initially, pomegranate peels (PP) were washed with deionized water and dried at room temperature for 48 hours. Following that, the dried pomegranate peels were crushed with pistil mortal and converted into fine powder. Three grams of pomegranate peel powder were then prepared for further characterization. Biogenic ZnO nanostructures were synthesized in the second phase using different amounts of prepared pomegranate peel powder: 2.22g $ZnC_4H_6O_4$ dissolved in 100 mL beakers and were designated Sample-1, Sample-2, and Sample-3. Pure ZnO is represented in the 1-beaker, which only contains $ZnC_4H_6O_4$. A preheated electric oven at 95 °C was used to bake the four glass beakers for five hours with aluminum foil covering them. A filter paper was then used to collect white biogenic ZnO samples. It was then annealed for 90 minutes at 200 °C.

2.3. Characterization of pure and biosynthesized ZnO nanostructures

X-ray diffraction patterns of synthesized nanostructures were analyzed using a Bruker D8 Advanced X-ray diffractometer (XRD) using CuK radiation (1.54050Å). A SEM JEOL-Jem was used to analyze the morphology of biogenic ZnO samples at a voltage of 15 kV. Lastly, the UV-vis spectrophotometer (PE Lamda 365) was used to determine how malachite green's absorption spectra changed with UV exposure.

2.4. Photocatalytic activity measurements

A photocatalytic experiment with Malachite green dye (MG) was conducted in quartz tubes exposed to sunlight with and without ZnO nanostructures. Typical photocatalytic degradation experiments involve the addition of 10 mg of catalyst to 50mL of dye MG aqueous solution with 13.70×10^{-5}M and 8.22×10^{-5}M. A certain period of time was then spent exposing the suspension to open sunlight. For the purpose of determining the amount of dye present before exposure to sunlight, a UV-visible spectrophotometer (PE Lamda365) was used to measure the absorption coefficient at a wavelength of 664 nm, which corresponds to the maximum absorbance of MG dye. Using the equation given below, we were able to calculate the dye removal (%) of MG.

Dye removal (%) = $\left(\frac{C_o - C_t}{C_o}\right)$*100

C_0 and C_t are the initial and final dye concentrations, respectively. Generally, the kinetics of heterogeneous photocatalysis can be modeled a pseudo-first-order reaction as follows:

$-\ln\frac{C_t}{C_o} = -k_{app}.t$

k_{pp} refers to the reaction rate kinetic constant of photocatalysis and t is the illumination time.

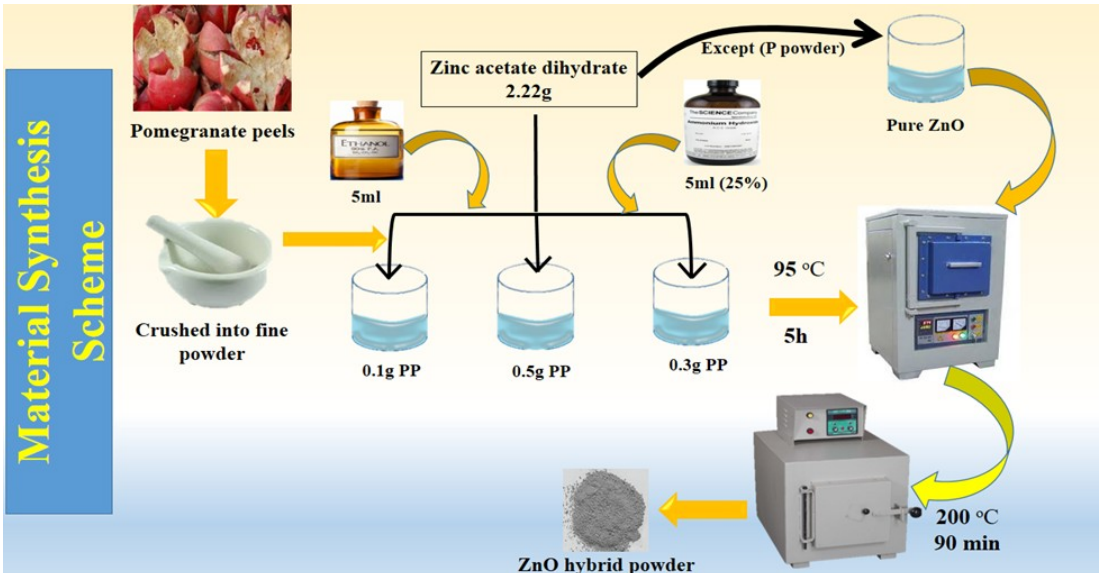

Scheme 2. Synthesis scheme of ZnO nanostructure using pomegranate peels powder.

3. Results and discussion

3.1. The structural characterization of ZnO nanostructures grown with the pomegranate peels powder

X-ray diffraction (XRD) was used to examine the influence of pomegranate peel powder on crystal phase, shift in two theta angle, and crystallite size. The measured distinctive diffraction patterns are shown in Figure 1. The effect of pomegranate peels powder on crystal quality is evident, and the relative intensity increases as the quantity of pomegranate peel powder increases. A variety of Miller Indices were observed and the typical crystal planes were (100), (002), (101), (102), (110), (103), (112) planes at their respective two theta angles. A standard JCPDS card number 01-97-0208 confirmed the hexagonal crystal phase. Pomegranate peel powder ontains phytochemicals which produce stress on the crystallization of ZnO nanostructures. This is demonstrated in Figure 1b, where a shift towards a higher angle is observed. Accordingly, it was determined that pomegranate peel powder had a significant effect on ZnO material by releasing phytochemicals during the synthesis. This resulted in crystal expansion, and thus certain crystal defects were induced. The XRD study revealed that the ZnO nanostructures are of high purity and that no other impurities can be detected since the measured diffraction patterns match those on the standard JCPDS card. In addition, the Scherrer Equation was used to calculate the crystallite size (Figure 1c). As illustrated in Figure 1c, increasing amounts of pomegranate peel powder have reduced the average crystallite size of ZnO nanostructures. In comparison with the samples 2, 1, and pure ZnO, sample 3 was found to have a smaller crystallite size of about 11 nm.

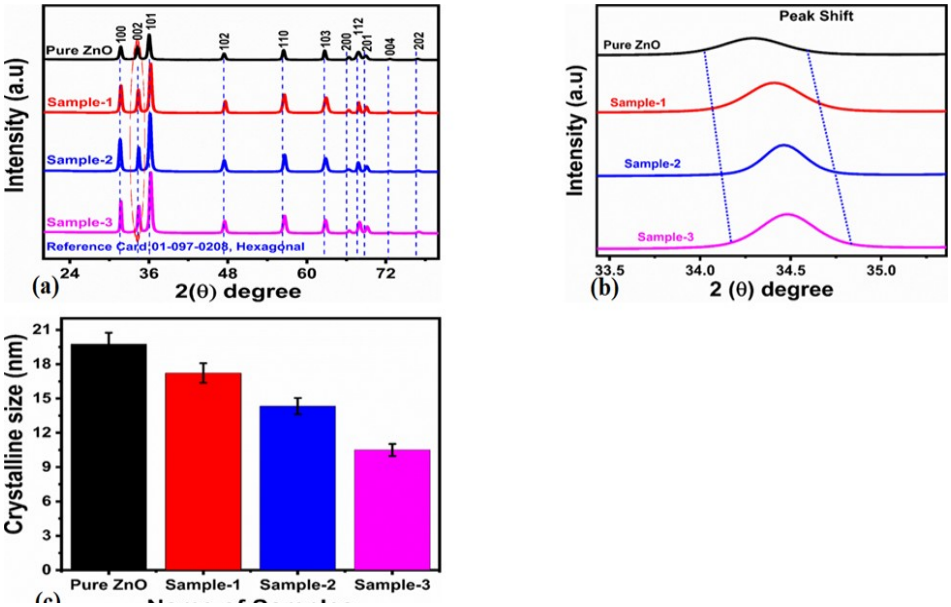

Figure 1. (a) XRD patterns of pure ZnO and green synthesized samples using different amount of pomegranate peel powder (0.3g, 0.5g and 1g), (b) showing the peak shift of synthesized pure ZnO and green synthesized samples (c) showing the crystalline size of different samples.

In Figure 2, scanning electron microscopy was used to examine the shape and structure of ZnO nanostructures in response to various amounts of pomegranate peel powder. Pure ZnO exhibited the typical randomly oriented nanorods with a diameter of less than 200 nm. Nevertheless, adding pomegranate peel powder resulted in the etching of nanorods, resulting in the surface becoming well reduced and the shape of ZnO nanostructures being significantly modified as shown in Figure 2b-d. The possible variation in the shape could be attributed to the presence of wide range of phytochemicals such as phenolic acids (hydroxycinnamic and hydroxybenzoic acids), flavonoids (anthocyanins, catechins, and other complex flavonoids) and hydrolysable tannins (ellagic and gallic acids, pedunculagin, punicalin and punicalagin in pomegranate peel (PP) [26, 27, 28]. In many cases, they were of the acidic nature, which etched the nanorods and showed the surface modification effect on the ZnO nanorods. It is further shown in Figure 2b-d that the presence of these phytochemicals in the pomegranate peel can significantly reduce, cap, and stabilize the shape disorder of ZnO nanostructures.

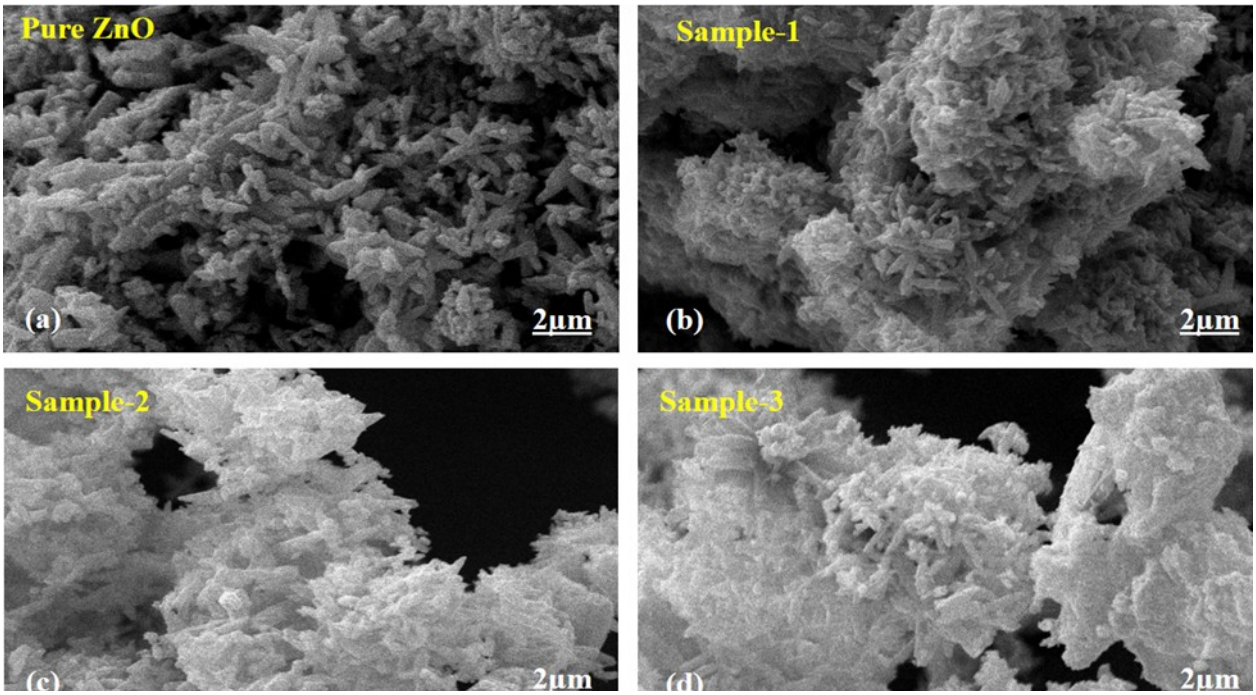

Figure 2. SEM morphology of hydrothermally assisted (a) pure ZnO and (b-d) showing the SEM morphology of green synthesized ZnO samples using different amount of pomegranate peels powder 0.3g, 0.5g and 1g.

A further method of understanding the chemical composition of ZnO nanostructures was accomplished by the use of energy dispersive spectroscopy (EDS). EDS analysis revealed only the typical signals associated with C, Zn, and O elements. However, the atomic percentage of zinc ions decreased with increasing amounts of pomegranate peel powder, as shown in Figure 3a-d. It appears that phytochemicals from pomegranate peel were used in the etching of ZnO along the zinc lattice.

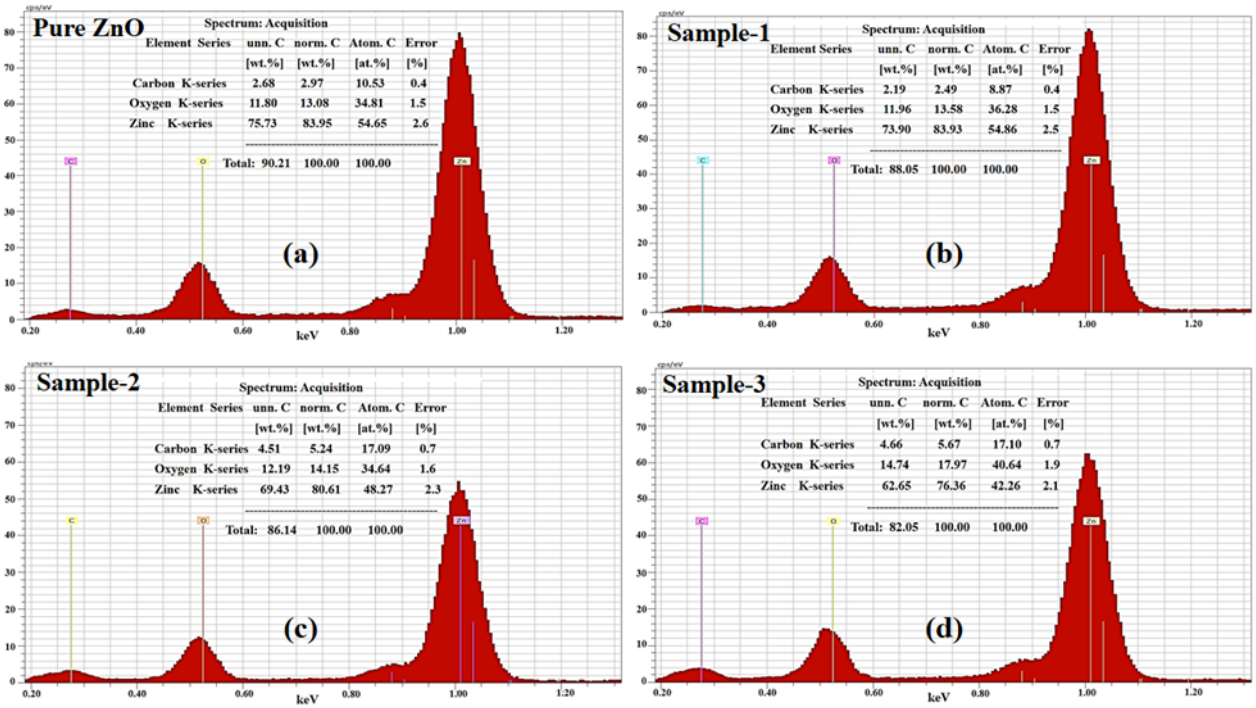

Figure 3. (a) EDS spectrum images of pure ZnO, and green synthesized ZnO samples using different amount of powder (b) 0.3g (c) 0.5g and (d) 1g of pomegranate peels.

A UV-visible spectrometer was used to evaluate the optical properties of ZnO nanostructures using pomegranate peel powder, as shown in Figure 4. In Figure 4, the measured absorbance in the region from

300-500 nm for each sample of ZnO is shown in relation to the quantity of pomegranate peel powder used. Furthermore, Tauc plots were simulated for optical band gap estimation as shown in Figure 4b. An analysis of the optical band gaps of each sample of ZnO was presented in Figure 4c as a bar graph. In Figure 4c, we can see that the optical band gap analysis revealed the role played by phytochemicals from pomegranate peel powder in reducing the band gap of sample-3 to 2.31 eV. Therefore, pomegranate peel powder offered highly efficient ZnO based photocatalysts for the degradation of malachite dye under sunlight.

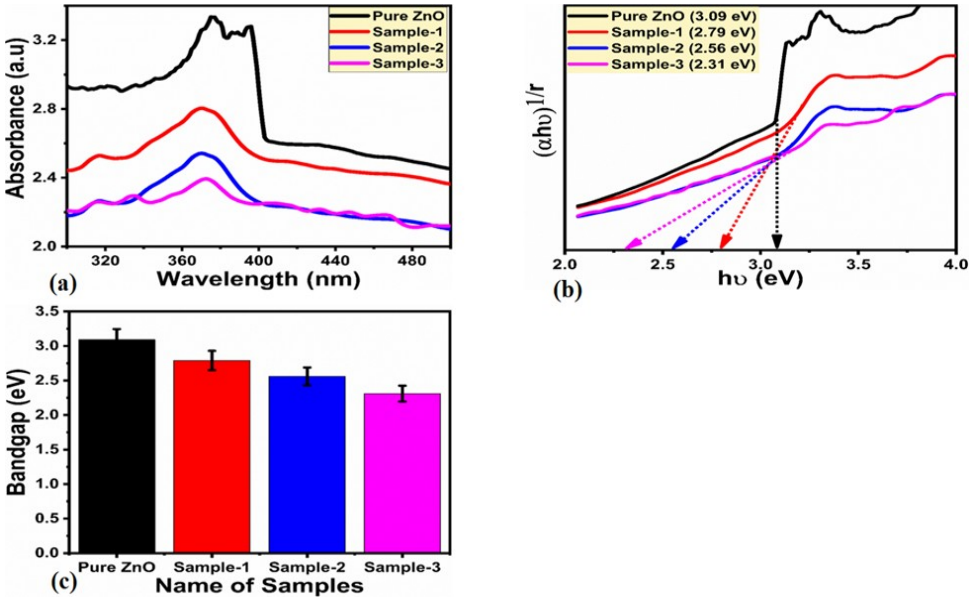

Figure 4. (a) Optical absorbance of synthesized samples (b) corresponding Kubelka-Munk plots (c) showing the bar graphs of band gap energies of pure ZnO and green synthesized ZnO samples.

3.2. Photocatalytic performance of as prepared ZnO nanostructures using pomegranate peel powder

In order to investigate the effect of sunlight on dye degradation, the dye concentration 13.70×10^{-5}M was illuminated with only natural sunlight before being subjected to the photocatalysis of malachite using the as prepared photocatalysts as shown in Figure 5. As shown in Figure 5, the UV-visible absorbance of dye shows negligible effects of sunlight on dye degradation when irradiated with photons as demonstrated by the negligible absorbance after 105 minutes of irradiation. In a similar manner, the light irradiation kinetics on malachite green were examined, with findings suggesting that the degradation rate was kinetically slow and the degradation of efficiency was less than 8%, as illustrated in Figures 5b and d. In the absence of photocatalysis dye degradation is negligible, therefore new photocatalysts are urgently required to effectively degrade dyes and address wastewater treatment challenges.

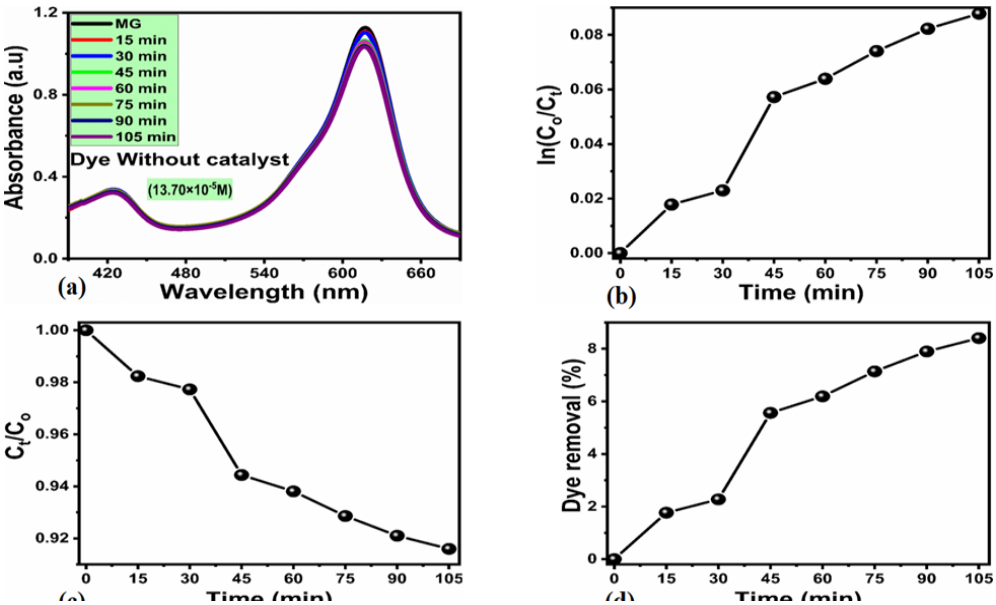

Figure 5. (a) Photocatalytic degradation of MG dye at concentration of 13.70×10^{-5}M without catalyst (b) calibration plot of ln(C_o/C_t) *vs* time for the degradation of MG dye (c) Ct/Co *vs* time for the degradation of MG and (c) calibration curve of dye removal (%) *vs* different time intervals under the sun light irradiation.

Consequently, ZnO has been identified as a potential degrader of synthetic dyes. Pure ZnO nanostructures were used towards the photodegradation of malachite green with varying concentration of 13.70×10^{-5}M and 8.22×10^{-5}M under the illumination of natural sunlight as shown in Figure 6a,b. After irradiation with natural sunlight at various intervals of time, the absorption spectra of dye degradation were recorded. Pure ZnO has shown relative low absorbance at high concentrations of malachite green than low malachite green concentrations, indicating the catalytic effect of ZnO is better at low concentrations due to greater interaction of sunlight photons with the surface ZnO and dye molecules. However, dye degradation continues to be a limiting factor since it takes a long time and limits the rate of photodegradation. When semiconducting ZnO was illuminated with sunlight while dye molecules were present, these aspects of limited kinetics were associated with the rapid recombination of electron-hole pairs, resulting in the electron-hole pairs being less effective in generating radical species capable of degrading the dye as a result of their fast recombination rates. As a result, these observations highlight the importance of studying ZnO with high efficiency for photocatalytic applications through the application of new synthetic strategies and material engineering techniques. However, the optical and surface properties of ZnO need to be improved in order to ensure that dye degradation occurs efficiently. Furthermore, the degradation kinetics of malachite green was also studied in its two different concentrations such as 13.70×10^{-5}M and 8.22×10^{-5}M as shown in Figure 6c-d. The rate constant value was higher for the low concentration than 13.70×10^{-5}M and it was following the pseudo first order kinetics. The reason for this is that the aqueous solution of dye contained a relatively small amount of dye relative to an excessive amount of water molecules, which meant that kinetics was primarily governed during the rate-determining step. Additionally, it was found that the kinetics at concentration was slow due to limited interaction of sunlight photons with ZnO surface because it was highly covered in dye molecules, which did not support the generation of large quantities of electrons and holes during light irradiation. According to Figure 6e, degradation efficiency was higher at low dye concentrations than at high dye concentrations. Approximately 54% of the degradation efficiency was observed at low concentrations while 33% was observed at high concentrations (Figure 6e). In the degradation of malachite under natural sunlight, pure ZnO showed limited decreases in absorbance of UV-visible spectra, slow kinetics, and low degradation efficiency. The results suggest that a new or modified synthetic method must be used to improve the surface, optical and crystalline properties of pure ZnO in order to improve its photocatalytic properties.

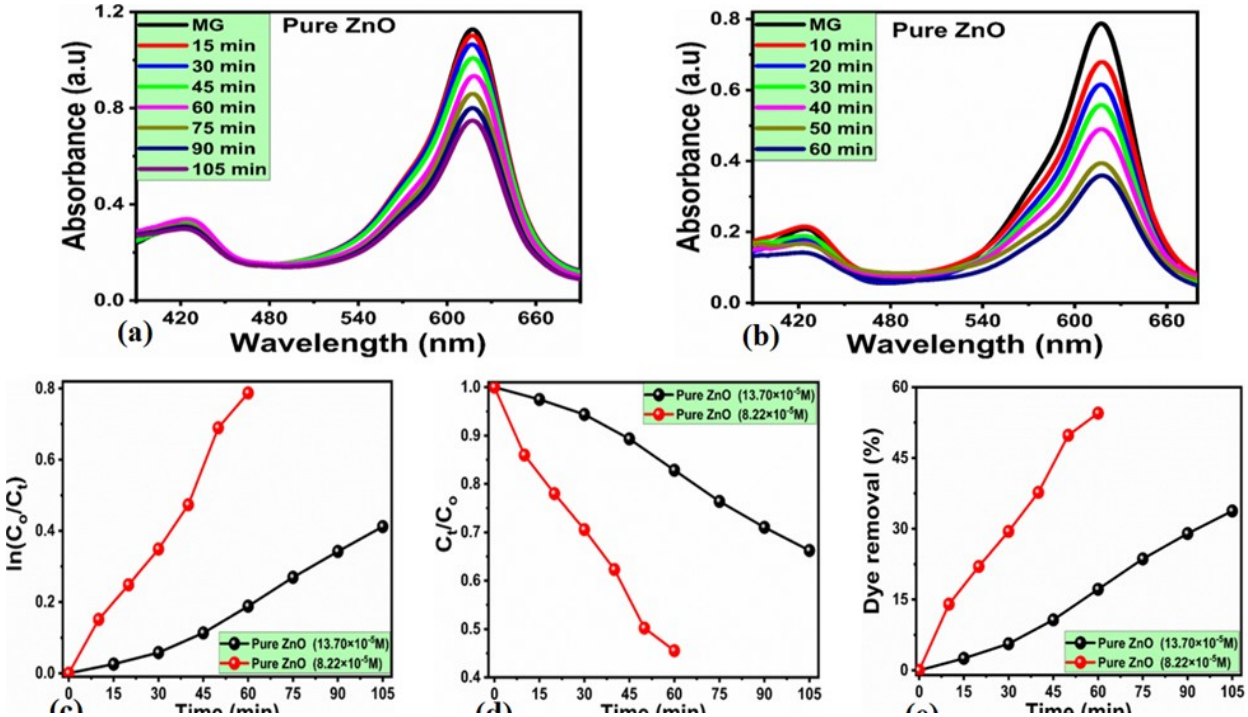

Figure 6. (a) Photocatalytic degradation of MG dye at concentration of 13.70×10^{-5}M using pure ZnO nanostructure under sun light irradiation of 105 min (b) Photocatalytic degradation of MG dye at concentration of 8.22×10^{-5}M using pure ZnO nanostructure under the sun light irradiation of 60 min (c) calibration plot of $\ln(C_o/C_t)$ *vs* time for the degradation of MG dye (c) Ct/Co *vs* time for the degradation of MG and (c) calibration curve of dye removal (%) *vs* different time intervals under the sun light irradiation .

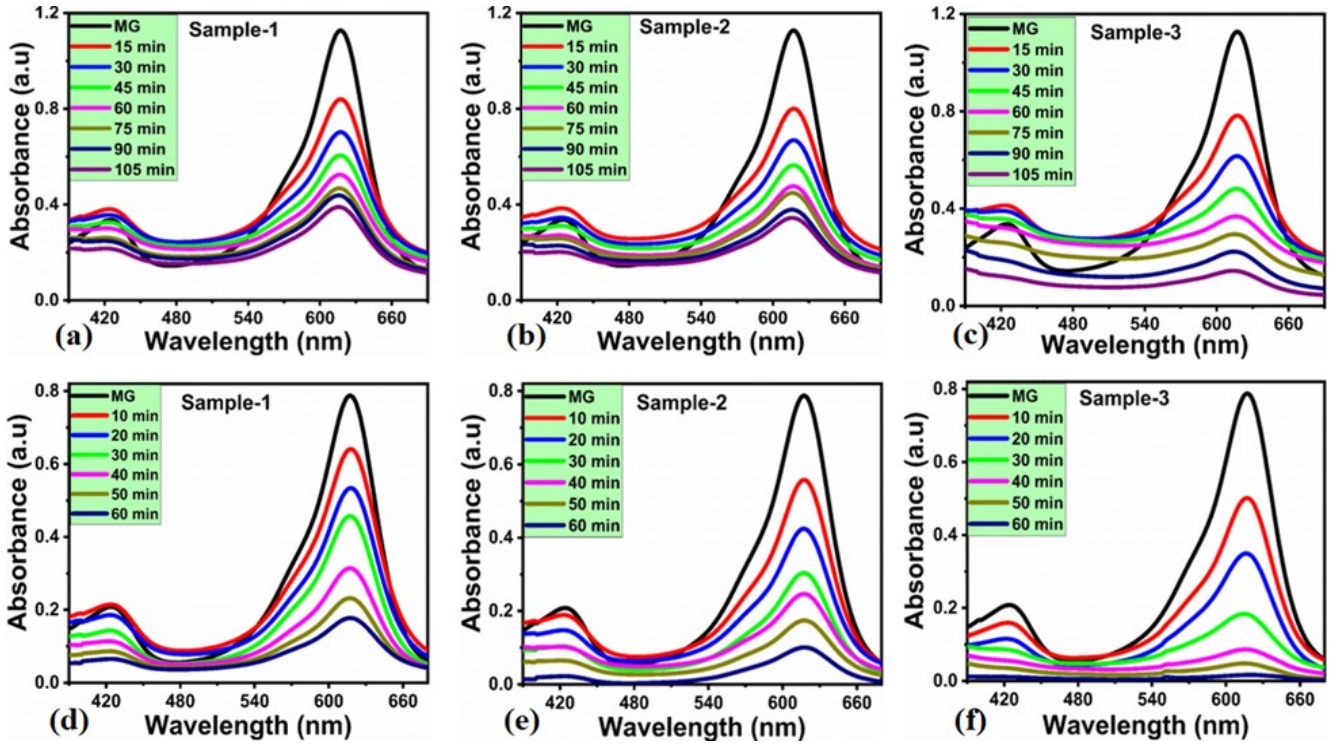

Figure 7. (a-c) Illustrate the Photocatalytic degradation of MG dye at concentration of 13.70×10^{-5}M using green synthesized ZnO samples under sun light irradiation and (d-f) showing the Photocatalytic degradation of MG dye at concentration of 8.22×10^{-5}M using green synthesized ZnO samples with different amount of pomegranate peel powder 0.3g, 0.5g and 1g under sun light irradiation of 60 min.

Because of this, we used pomegranate peel powder to grow ZnO, which supplied a significant amount of phytochemicals that reduced, capping, and stabilized ZnO. This contributed greatly to the structural

deformation, increased crystal quality, enhanced active sites, and reduced optical band gap, all of which have proven to be highly useful during outstanding photocatalytic properties. In Figure 7, malachite green concentrations of 13.70×10^{-5}M and 8.22×10^{-5}M were applied to a variety of ZnO samples prepared with pomegranate peel powder and irradiated in natural sunlight with the same amount of catalyst dose of 15 mg. In Figure 7a-c, we are able to see a decrease in the UV-visible absorbance spectra in high concentrations of malachite green 13.70×10^{-5}M. As compared to pure ZnO, surface modified ZnO nanostructures containing pomegranate peel powder showed a significant decrease in absorbance of malachite green, indicating that phytochemicals have an impact on the photocatalytic activity of ZnO. ZnO samples prepared with different quantities of pomegranate peel powder, however, showed a greater ability to photocatalyze malachite green at low concentrations (8.22×10^{-5}M) as illustrated in Figures 7d-f. Because less dye molecules were crowded on the surface of ZnO at a low concentration of 8.22×10^{-5}M, there was an enhanced catalytic activity. As a result of the high interaction of photons from sunlight, a large number of electrons and holes were generated, resulting in more radicals which were beneficial to the degradation of malachite green in aqueous solution, for example. As a result of high concentrations of 13.70×10^{-5}M, the dye molecules may have formed a thick layer on the surface of ZnO, which prevented photons from interacting with it. Due to the smaller number of electrons and holes generated, a significant amount of radical species were not added, which were further involved in the degradation process of the dye. Therefore, modified ZnO samples perform relatively poorly in high concentrations of malachite green 13.70×10^{-5}M as compared to low concentrations. Furthermore, Figure 8 illustrates the kinetics of malachite green under natural sunlight illumination in high concentrations of 13.70×10^{-5}M and in low concentrations of 8.22×10^{-5}M. Figure 8a-c illustrates the kinetics of malachite degradation at high concentrations of 13.70×10^{-5}M for sample 1, sample 2, and sample 3. It was found that the degradation rate of modified ZnO was significantly higher than the degradation rate of pure ZnO, as indicated by the high rate constant values, and the degradation kinetics followed the pseudo-first order model. The rate constant values for sample 1, sample 2 and sample 3 in high concentration were as 0.00955 min^{-1}, 0.0105 min^{-1}, 0.0185min^{-1} respectively. Samples 3 and 2 were found to have a higher degradation efficiency due to the highly modified surfaces, low optical band gaps, and crystallite sizes, as compared to samples 1 and 2. It can be seen that the kinetic effect of malachite green is greater at low concentrations of 8.22×10^{-5}M for samples 1, 2 and 3, as observed in Figure 8d-f, which shows a high rate constant value compared to high concentrations of malachite green. Rate constant values for the sample 1, sample 2, and sample 3 as 0.024 min^{-1}, 0.032 min^{-1}, and 0.063 min^{-1} respectively in low concentration of malachite green. Meanwhile, the degradation efficiency for sample 3 was found to be almost 97.67% in 60 minutes, which is a very short time interval. Based on these kinetic studies in low and high concentrations, it appeared that surface modified ZnO was capable of outperforming dye degradation efficiency within a very short period of time.

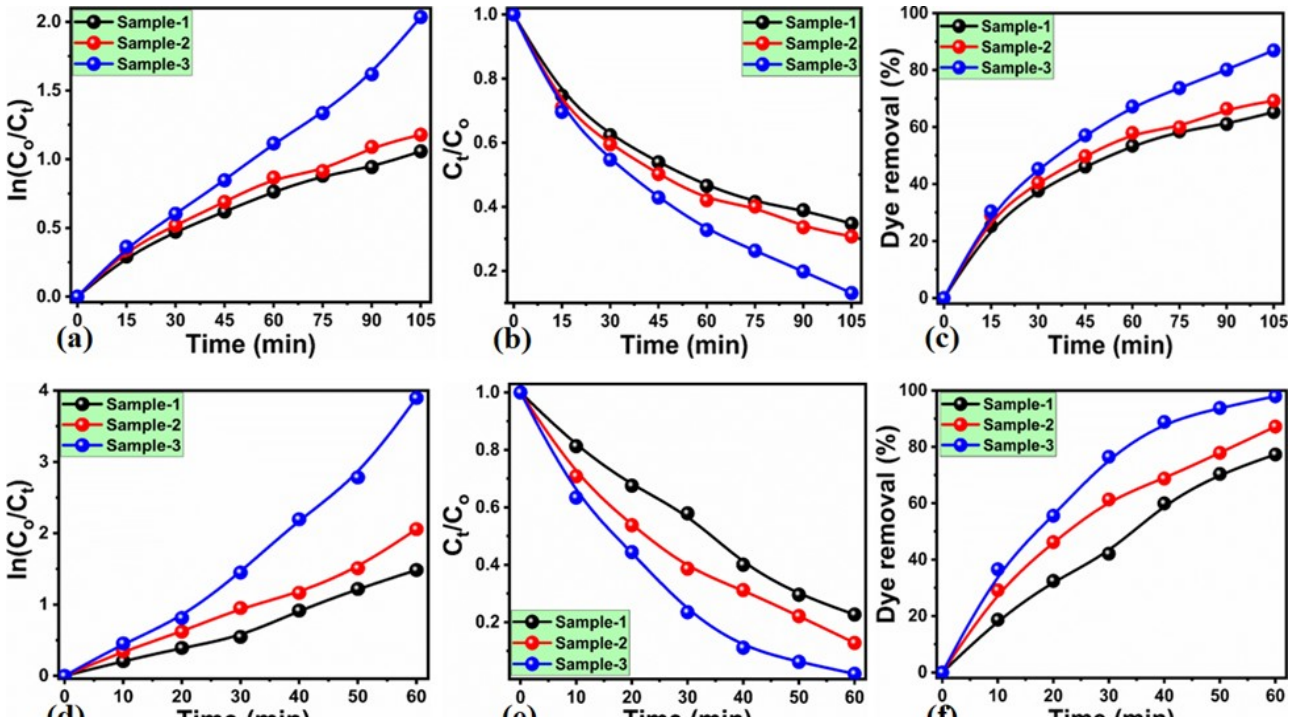

Figure 8. (a) calibration plot of ln(C_o/C_t) *vs* time for the degradation of MG dye at concentration of 13.70×10^{-5}M under sun irradiation of 105 min (b) Ct/Co *vs* time for the degradation of MG and (c) calibration curve of MG dye removal (%) *vs* different time intervals under the sun light irradiation of 105 min. (d) calibration plot of ln(C_o/C_t) *vs* time for the degradation of MG dye at concentration of 8.22×10^{-5}M under sun irradiation of 60 min (e) Ct/Co *vs* time for the degradation of MG and (f) calibration curve of MG dye removal (%) *vs* different time intervals under the sun light irradiation of 60 min. .

Figure 9a-c illustrates the effect of pH on the photocatalytic performance of the ZnO based photocatalyst prepared with high quantities of pomegranate peel powder. With the assistance of concentrated NaOH and HCl in aqueous solution, three pH values such as 3, 7 and 11 were adjusted in the dye solution of 13.70×10^{-5}M. Several factors affect the degradation kinetics of ZnO nanostructures depending on pH, including variations in hydroxyl radicals and changes in charge on the surface of ZnO nanostructures [29, 30, 31]. As part of each pH adjustment dye solution, the catalyst dose of 10 mg was used and the solution was irradiated with natural sunlight. In Figures 9a-c, a decrease in absorbance was observed for each dye solution adjusted to pH 3, 7 and 11. Upon examining Figure 9c, it is evident that the dye degradation efficiency remained 97.14% at pH 11 after a short interval of time of 20 minutes. Depending on the pH of the dye solution, variations in charge are generated on the surface of ZnO, which may further attract dye molecules. The pHpzc (point of zero charge) for pure ZnO was observed to be 8.1 [32], while the pHpzc of the newly developed photocatalyst of ZnO with pomegranate peel powder was 9.8. The pHpzc value below 8.3 indicates that the surface is likely to be positively charged. However, for pHpzc values greater than 8.3, is a sign of highly negative surfaces on as prepared ZnO samples, which can effectively degrade cationic dyes because the negatively charged surface is capable of attracting the positively charged dyes. The degradation is therefore expected to be effective. According to Figure 9d-e, the pH has significantly accelerated the kinetics as demonstrated by the large rate constant value of 0.159 min^{-1} at pH 11, 0.0688 min^{-1}, 0.0337 min^{-1} at pH 3 and the degradation kinetics follow pseudo first order kinetics for pH 3, 7 and 11. In Figure 9f, the degradation efficiency was found to be about 97.14% for pH 11, 91% for pH 7, and 44.30% for pH 3. The degradation efficiency was low at pH 3 due to the repletion between hydronium ions and positively charged malachite dye molecules, thus there was less likely interaction between the ZnO surface and the dye. Contrary to pH 11, the degradation was due to a highly negative surface of ZnO which showed efficient interaction between the dye molecules and the surface of ZnO. As a result of the abundance of hydroxyl ions at pH 11, hydroxyl radicals were generated through the interaction of electron-hole pairs generated under solar radiation, resulting in efficient dye degradation rates.

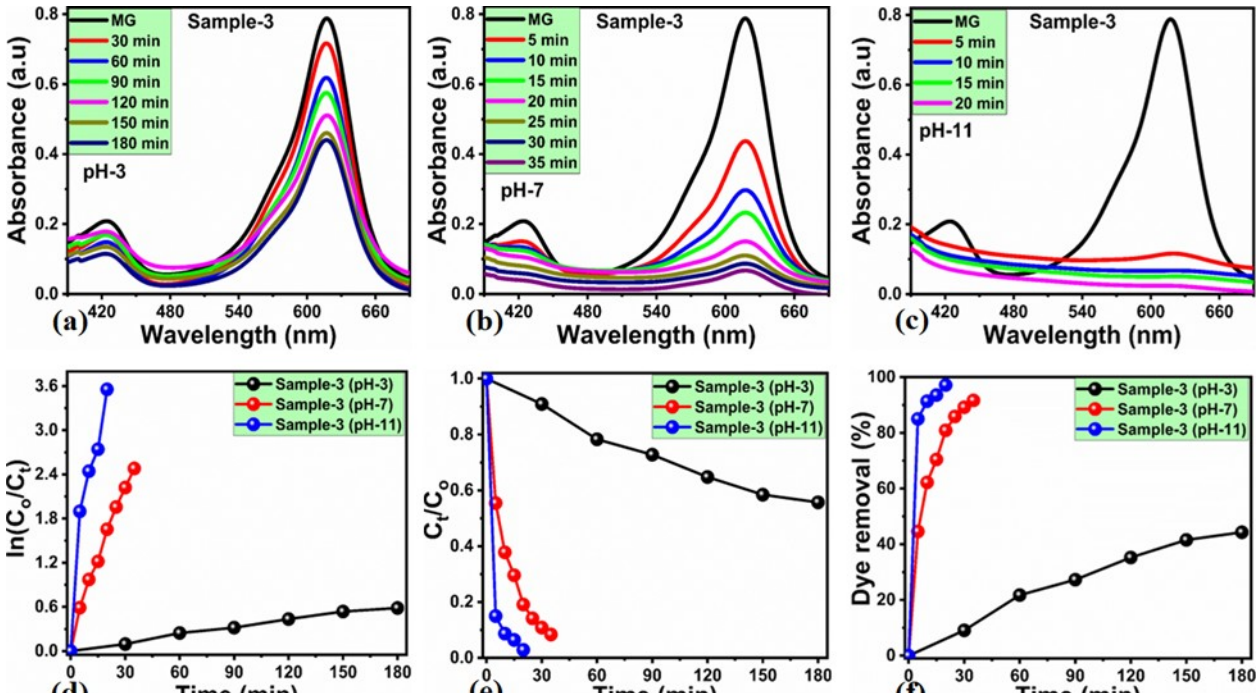

Figure 9. Photocatalytic degradation of MG dye at concentration of 8.22×10^{-5}M using green synthesized ZnO samples at different pH values of (a) pH-3, (b) pH-7 and (c) pH-11 at different time interval of 180min, 35min and 20 min. (d) calibration plot of $\ln(C_o/C_t)$ *vs* time for the degradation of MG dye at concentration of 8.22×10^{-5}M under sun irradiation of 180 min, 35 min and 20 min (e) Ct/Co *vs* time for the degradation of MG and (f) calibration curve of MG dye removal (%) *vs* different time intervals under the sun light irradiation at different pH values. .

The reusability of ZnO nanostructures prepared with highest amount of pomegranate peel powder (sample 3) using 10 mg of catalyst was investigated for six repeatable degradation cycles in 8.22×10^{-5}M under the illumination of natural sunlight as shown in Figure 10. Prior to the reusability 0 cycle was labeled as control experiment as shown in Figure 10. After repetition of six degradation cycles, the degradation efficiency was still significant, indicating the material stability.

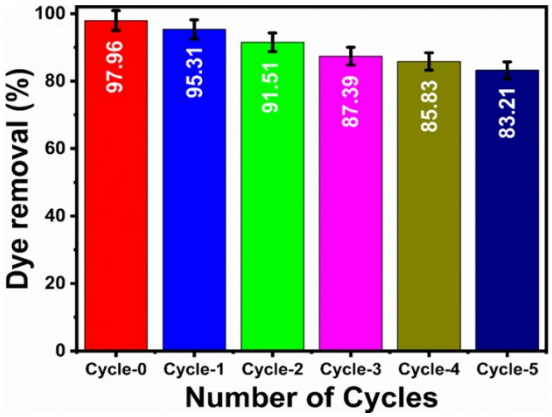

Figure 10. The reusability test of ZnO nanostructures against the photodegradation of malachite green 8.22×10^{-5}M prepared with highest amount of pomegranate peel powder (sample 3) under the illumination of natural sunlight.

Using ZnO nanostructures prepared from pomegranate peel powder, a scavenger study was conducted to identify possible radicals that are involved in malachite green degradation, as shown in Figure 11. We employed various scavengers including ascorbic acid, ethylenediamine tetracetate (EDTA), and sodium borohydride to inhibit malachite green degradation at 8.22×10^{-5}M concentration in an environment where natural sunlight was irradiated. Scavenger agents were diluted to a concentration of 12 mM and mixed with dye solution that contained 8.22×10^{-5}M. It has generally been established that dye degradation occurs due to radicals such as superoxide ($\cdot O_2$), hydroxyl ($\cdot OH$), and high electron-hole pairing density. Particularly, dye

degradation is dominated by superoxide ($\cdot O_2$), hydroxyl ($\cdot OH$) radicals as reported in several studies [33, 34, 35]. The presented study revealed that the degradation efficiency of malachite green was highly inhibited in the presence of EDTA. This confirms the major role of hydroxyl radicals involved in malachite green degradation as shown in Figure 11.

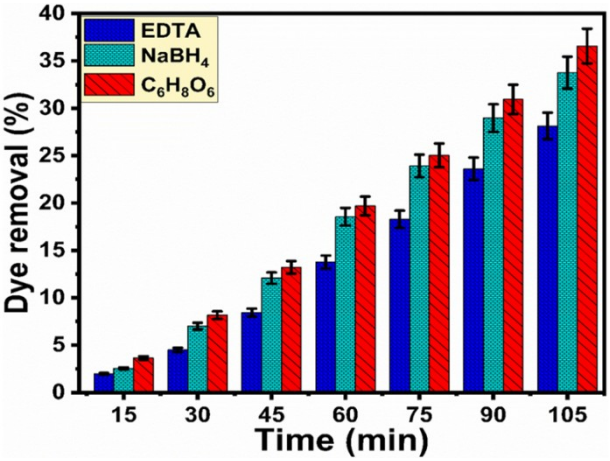

Figure 11. Dye removal (%) of MG under sun light irradiation using different scavengers at MG concentration of 8.22×10^{-5}M using a catalyst dose of 10mg under sun light irradiation.

ZnO and malachite green molecules undergo reduction and oxidation as part of the degradation mechanism. The ZnO nanostructures prepared from pomegranate peel powder exhibit semiconducting properties when they are irradiated with the surface of ZnO and electron and hole pairs are formed. Afterwards, these holes interact with water and generate hydroxyl free radicals, which are subsequently captured by oxygen molecules resulting from superoxide. Through the interaction between these free radicals and the superoxide, the dye is degraded into harmless mineralized products. The following are the general steps involved in the degradation process.

$$ZnOPP + hv \rightarrow e^- + h^+ \quad (1)$$

$$h^+ + H_2O \rightarrow O^{\bullet}H + h^+ \quad (2)$$

$$h^+ + OH^- \rightarrow O^{\bullet}H \quad (3)$$

$$e^- + O_2 \rightarrow O_2^{\bullet -} \quad (4)$$

$$h^+ + H_2O \rightarrow O^{\bullet}H + h^+ \quad (5)$$

$$O^{\bullet}H + \text{malachite green} \rightarrow \text{Mineralized products} \quad (6)$$

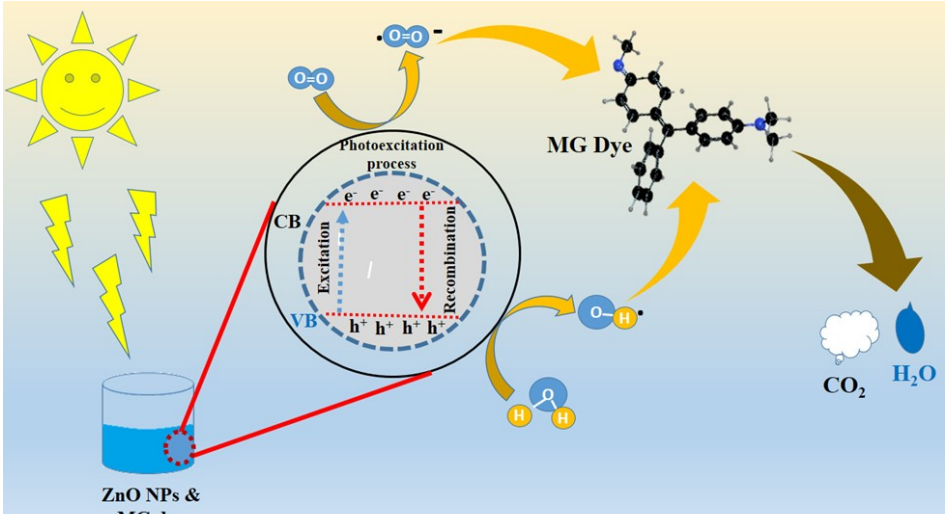

Scheme 3. General photodegradation of mechanism of dye onto semiconducting ZnO material prepared with pomegranate peel powder.

The performance evaluation of as prepared ZnO nanostructures with the pomegranate peel powder (sample 3) was carried out with the reported results on photodegradation of malachite green as given in Table 1. It is obvious that the presented results in terms of high photodegradation efficiency are superior even at high concentration of malachite green compare to the recently reported results.

Table 1. Comparison of photodegradation percentage of synthesized ZnO nanostructures for MG with previously reported study.

Catalysts	MG Dyes concentration	Time(min)	Removal %	Reference
Biosynthesized ZnO NPs	4.56 × 10−5 M	160	91.2	36
ZEDTA	1 × 10−5 M	61	94.14	37
CDC	2.18 × 10−5 M	90	93	38
ZnO–NPs	10.96×10^{-5}M	120	85.3	39
$CeFeO_3$	2 × 10–5 M	120	91	40
L-CMTS	0.72 × 10–5 M	140	95	41
$CoMn_2O_4$	1.370 × 10−5 M	60	87	42
$ZnO/GdCoO_3$	6.0 × 10−6 M	120	92.4	43
Biosynthesized ZnO NPs	4.56 × 10−5 M	160	91.2	44
ZnO NPs	1.5 mg/l	60	92	45
CoCA	1×10^{-5} M	100	91.2	46
ZnO / pomegranate peel powder	8.22×10^{-5}M	60	97.96	**Present work**

4. Conclusions

We have prepared ZnO nanostructures using pomegranate peel powder via a low temperature aqueous chemical synthesis method using the green synthesis method. A variety of amounts of pomegranate peel powder were used in order to modify the surface, optical, and crystalline properties of ZNO nanostructures. Pomegranate peel powder contains a diverse range of phytochemicals that may act as capping, reducing, and stabilizing agents to control ZnO size and optical characteristics. Nanostructures of ZnO were characterized by SEM, XRD, EDS, and UV-visible spectroscopy. A study has also been conducted to evaluate the role of pomegranate peel powder in the photodegradation of malachite green under natural sunlight illumination. A ZnO sample prepared with the highest amount of pomegranate peel powder degraded dye almost 97.96% at a low concentration of malachite green. It was shown that pomegranate peel powder could be used to create various metal oxide nanostructures for the development of new electrocatalysts/photocatalysts for clean energy and environmental issues.

Acknowledgment: The authors would like to acknowledge the Higher Education Commission of Pakistan for its partial support of the project (NRPU/8350). The authors extend their sincere appreciation to the Researchers Supporting Project number (RSP2023R79), King Saud University, Riyadh, Saudi Arabia, for partial fund-ing of this work. The authors acknowledge partial funding from Ajman University, Grant DRGS Ref: 2022-IRG-HBS-9.

Conflicts of Interest: Authors have no conflict of interest in the presented research work.

References

[1]. Suresh, D.; Nethravathi, P.C.; Rajanaika, H.; Nagabhushana, H.; Sharma, S.C. Green synthesis of multifunctional zinc oxide (ZnO) nanoparticles using Cassia fistula plant extract and their photodegradative, antioxidant and antibacterial activities. Materials Science in Semiconductor Processing. **2015,** 31, 446-54.

[2]. Podasca, V.E.; Damaceanu, M.D. Photopolymerized films with ZnO and doped ZnO particles used as efficient photocatalysts in malachite green dye decomposition. Applied Sciences. **2020,** 6, 1954.

[3]. Srivastava, S.; Sinha, R.; Roy, D. Toxicological effects of malachite green Aquat. Toxicol. **2004,** 66, 319-329.

[4]. Chauhan, A.K.; Kataria, N.; Garg, V.K. Green fabrication of ZnO nanoparticles using Eucalyptus spp. Leaves extract and their application in waste-water remediation, Chemosphere, **2020,** 247, 125803.

[5]. Sun, J.H.; Sun, S.P.; Wang, G.L.; Qiao, L.P. Degradation of azo dye Amido black 10B in aqueous solution by Fenton oxidation process. Dyes and pigments. **2007,** 74, 647-52.

[6]. Etacheri, V.; Roshan, R.; Kumar, V. Mg-doped ZnO nanoparticles for efficient sunlight driven photocatalysis, ACS Appl. Mater. Interfaces, **2012,** 4, 2717-2725.

[7]. Zhang, Y.; Lu, J.; Hoffmann, M.R.; Wang, Q.; Cong, Y.; Wang, Q.; Jin, H. Synthesis of g-C 3 N 4/Bi 2 O 3/TiO 2 composite nanotubes: enhanced activity under visible light irradiation and improved photoelectrochemical activity, RSC Adv., **2015,** 5, 48983-48991.

[8]. Hernández, S.; Hidalgo, D.; Sacco, A.; Chiodoni, A.; Lamberti, A.; Cauda, V.; Tresso, E.; Saracco, G. Comparison of photocatalytic and transport properties of TiO 2 and ZnO nanostructures for solar-driven water splitting, Phys. Chem. Chem. Phys., **2015,** 17, 7775-7786.

[9]. Zamiri, R.; Ahangar, H.A.; Tobaldi, D.M.; Rebelo, A.; Seabra, M.P.; Shabani, M.; Ferreira, J.M.F. Fabricating and characterising ZnO–ZnS–Ag 2 S ternary nanostructures with efficient solar-light photocatalytic activity. *Physical Chemistry Chemical Physics*, **2014,** 40, 22418-22425.

[10]. Kamat, P.V. Meeting the clean energy Demand: nanostructure architectures for solar energy conversion, J. Phys. Chem. C, **2007,** 111, 2834-2860

[11]. Willander, M.; Nur, O.; Zhao, Q.X.; Yang, L.L.; Lorenz, M.; Cao, B.Q.; Pérez, J.Z.; Czekalla, C.; Zimmermann, G.; Grundmann, M.; Bakin, A.; Behrends, A.; Al-Suleiman, M.; El-Shaer, A.; Mofor, A.C.; Postels, B.; Waag, A.; Boukos, N.; Travlos, A.; Kwack, H.S.; Guinard, J.; Dang, D.L.S. Zinc oxide nanorod based photonic devices: recent progress in growth, light emitting diodes and lasers, Nanotechnology, **2009,** 20, 332001.

[12]. Moussa, H.; Girot, E.; Mozet, K.; Alem, H.; Medjahdi, G.; Schneider R. ZnO rods/reduced graphene oxide composites prepared via a solvothermal reaction for efficient sunlight-driven photocatalysis, Appl. Catal. B Environ., **2016,** 185, 11-21.

[13]. Paula, C.H.R.; Andrade Neto, N.F.; Garcia, L.M.P.; Nascimento, R.M.; Paskocimas, C.A.; Bomio, M.R.D.; Motta, F.V. Increased degradation capacity of methylene blue dye using Mg-doped ZnO nanoparticles decorated by Ag0 nanoparticles, J. Electron. Mater., **2019,** 48, 3017-3025.

[14]. Baruah, S.; Sinha, S.S.; Ghosh, B.; Pal, S.K.; Raychaudhuri, A.K.; Dutta, J. Photoreactivity of ZnO nanoparticles in visible light: effect of surface states on electron transfer reaction, J. Appl. Phys., **2009,** 105, 074308.

[15]. Sitthichai, S.; Phuruangrat, A.; Thongtem, T.; Thongtem, S. Influence of Mg dopant on photocatalytic properties of Mg-doped ZnO nanoparticles prepared by sol–gel method, J. Ceram. Soc. Jpn., **2017,** 125, 122-124.
[16]. Nouri, H.; Habibi-Yangjeh, A. Microwave-assisted method for preparation of Zn1−xMgxO nanostructures and their activities for photodegradation of methylene blue, Adv. Powder Technol., **2014,** 25, 1016-1025.
[17]. Kaliraj, L.; Ahn, J.C.; Rupa, E.J.; Abid, S.; Lu, J.; Yang, D.C. Synthesis of panos extract mediated ZnO nano-flowers as photocatalyst for industrial dye degradation by UV illumination. *Journal of Photochemistry and Photobiology B: Biology*, **2019,** *199*, 111588.
[18]. Chung, Y.T.; Ba-Abbad, M.M.; Mohammad, A.W.; Hairom, N.H.H.; Benamor, A. Synthesis of minimal-size ZnO nanoparticles through sol–gel method: Taguchi design optimisation. *Materials & Design*, **2015,** *87*,780-787.
[19]. Lastra, G.; Luque, P.A.; Quevedo-Lopez, M.A.; Olivas, A. Electrical properties of p-type ZnTe thin films by immersion in Cu solution. *Materials Letters*, **2014,** *126*, 271-273.
[20]. Patil, N.B.; Nimbalkar, A.R.; Patil, M.G. ZnO thin film prepared by a sol-gel spincoating technique for NO2 detection, Mater. Sci. Eng. B, **2018,** 227, 53-60.
[21]. Alharthi, F.A.; Alghamdi, A.A.; Alothman, A.A.; Almarhoon, Z.M.; Alsulaiman, M.F.; Al-Zaqri, N. Green synthesis of ZnO nanostructures using Salvadora Persica leaf extract: applications for photocatalytic degradation of methylene blue dye. *Crystals*, **2020,** *10*, 441.
[22]. Golmohammadi, M.; Honarmand, M.; Ghanbari, S. A green approach to synthesis of ZnO nanoparticles using jujube fruit extract and their application in photocatalytic degradation of organic dyes, Spectrochim. Acta A. Mol. Biomol. Spectrosc., **2020,** 229,117961.
[23]. Mirzaei, H.; Darroudi, M. Zinc oxide nanoparticles: biological synthesis and biomedical applications, Ceram. Int., **2017,** 43, 907-914.
[24]. Shabaani, M.; Rahaiee, S.; Zare, M.; Jafari, S.M. Green synthesis of ZnO nanoparticles using loquat seed extract; Biological functions and photocatalytic degradation properties. *Lwt*, **2020,** *134*, 110133.
[25]. Rambabu, K.; Bharath, G.; Banat, F.; Show, P.L. Green synthesis of zinc oxide nanoparticles using Phoenix dactylifera waste as bioreductant for effective dye degradation and antibacterial performance in wastewater treatment. *Journal of hazardous materials*, **2021,** *402*, 123560.
[26]. Singh B.; Singh J.P.; Kaur A.; Singh N. Phenolic compounds as beneficial phytochemicals in pomegranate (Punica granatum L.) peel: A review. Food Chem. **2018,** 261, 75–86.
[27]. Pirzadeh, M.; Caporaso, N.; Rauf, A.; Shariati, M.A.; Yessimbekov, Z.; Khan, M.U.; Imran, M.; Mubarak, M.S. Pomegranate as a source of bioactive constituents: A review on their characterization, properties and applications. Crit. Rev. Food Sci. Nutr. **2020,** 0, 1–18.
[28]. Bar-Ya'akov, I.; Tian, L.; Amir, R.; Holland D. Primary metabolites, anthocyanins, and hydrolyzable tannins in the pomegranate fruit. Front. Plant Sci. **2019,** 10, 1–19.
[29]. Marathe, Y.V.; Ramanna, M.M.V.; Shrivastava, V.S. Synthesis and characterization of nanocrystalline CdS thin films grown by chemical bath deposition at different molarities for removal of methylene blue. *Desalin Water Treat.* **2013,** *51*, 5813–5820.
[30]. Shanthi, M.; Kuzhalosai, V. Photocatalytic degradation of an azo dye, Acid Red 27, in aqueous solution using nano ZnO. *Ind. J. Chem.* **2012,** *51*, 428–434.
[31]. Mohammadzadeh, S.; Olya, M.E.; Arabi, A.M.; Shariati, A.; Khosravi, N.M.R. Synthesis, characterization and application of ZnO–Ag as a nanophotocatalyst for organic compounds degradation, mechanism and economic study. *J. Environ. Sci.* **2015,** *35*, 194–207.
[32]. Jakhrani, M.A.; Bhatti, M.A.; Tahira, A.; Shah, A.A.; Dawi, E.A.; Vigolo, B.; Nafady, A.; Saleem, L.M.; Haj Ismail, A.A.K.; Ibupoto, Z.H. Biogenic Preparation of ZnO Nanostructures Using Leafy Spinach Extract for High-Performance Photodegradation of Methylene Blue under the Illumination of Natural Sunlight. *Molecules*, **2023,** *28*, 2773.
[33]. Fatehah, M.O.; Aziz, H.A.; Stoll, S. Stability of ZnO nanoparticles in solution, influence of pH, dissolution, aggregation and disaggregation effects. *J. Colloid Sci. Biotechnol.* **2014,** *3*, 75–84.
[34]. Farrokhi, M.; Hosseini, S.; Yang, J.; Shirzad-Siboni, M. Application of ZnO–Fe_3O_4 nanocomposite on the removal of azo dye from aqueous solutions: Kinetics and equilibrium studies. *Water Air Soil Pollut.* **2014,** *225*, 1–12.
[35]. Akpan, U.G.; Hameed, B.H. Parameters affecting the photocatalytic degradation of dyes using TiO_2-based photocatalysts: A review. *J. Hazard. Mater.* **2009,** *170*, 520–529.
[36]. Bhatti, M.A.; Tahira, A.; Chandio, A.D.; Almani, K.F.; Bhatti, A.L.; Waryani, B.; Nafady, A.; Ibupoto, Z.H., Enzymes and phytochemicals from neem extract robustly tuned the photocatalytic activity of ZnO for the degradation of malachite green (MG) in aqueous media. *Research on Chemical Intermediates*, **2021,** *47*, 1581-1599.
[37]. Meena, S.; Vaya, D.; Das, B.K. Photocatalytic degradation of Malachite Green dye by modified ZnO nanomaterial. *Bulletin of Materials Science*. **2016,** *39*, 1735-1743.
[38]. Amar, I.A.; Harara, H.M.; Baqul, Q.A.; Abdul Qadir, M.A.; Altohami, F.A.; Ahwidi M.M.; Abdalsamed, I.A.; Saleh, F.A.; Photocatalytic degradation of malachite green dye under UV light irradiation using calcium-doped ceria nanoparticles. *Asian Journal of Nanosciences and Materials*. **2020,** *3,* 1-14.

[39]. Bhatti, M.A.; Tahira, A.; Hullio, A.A.; Aftab, U.; Nafady, A.; Vigolo, B.; Ibupoto, Z.H. Oxygenated terminals of milky sap of Calotropis procera transformed 1D ZnO structure to 0D nanoparticles for enhanced photocatalytic degradation of malachite green and methylene blue. *Journal of Materials Science: Materials in Electronics*, **2023,** *34*, 929.

[40]. Ameta, K.L.; Papnai, N.; Ameta, R. Photocatalytic degradation of Malachite Green using nano-sized cerium-iron oxide. *Orbital: The Electronic Journal of Chemistry*. **2014,** *6*, 14-19.

[41]. Malik, J.H.; Zaman, M.B.; Poolla, R.; Malik, K.A.; Assadullah, I.; Bhat, A.A.; Tomar, R. Hydrothermal synthesis of tetragonal and wurtzite Cu2MnSnS4 nanostructures for multiple applications: Influence of different sulfur reactants on growth and properties. *Materials Science in Semiconductor Processing*. **2021,** 121, 105438.

[42]. Mark, J.A.; Venkatachalam, A.; Pramothkumar, A.; Senthilkumar, N.; Jothivenkatachalam, K.; prince Jesuraj, J. Investigation on structural, optical and photocatalytic activity of CoMn2O4 nanoparticles prepared via simple co-precipitation method. *Physica B: Condensed Matter*. **2021,** 601, 412349.

[43]. Yulizar, Y.; Eprasatya, A.; Apriandanu, D.O.; Yunarti, R.T. Facile synthesis of ZnO/GdCoO3 nanocomposites, characterization and their photocatalytic activity under visible light illumination. *Vacuum*. **2021,** 183, 109821.

[44]. Bhatti, M.A.; Tahira, A.; Almani, K.F.; Bhatti, A.L.; Waryani, B.; Nafady, A.; Ibupoto, Z.H. Enzymes and phytochemicals from neem extract robustly tuned the photocatalytic activity of ZnO for the degradation of malachite green (MG) in aqueous media. *Research on Chemical Intermediates*. **2021,** 47, 1581-1599.

[45]. Ekennia, A.C.; Uduagwu, D.N.; Nwaji, N.N.; Oje, O.O.; Emma-Uba, C.O.; Mgbii, S.I.; Olowo, O.J.; Nwanji, O.L. Green synthesis of biogenic zinc oxide nanoflower as dual agent for photodegradation of an organic dye and tyrosinase inhibitor. *Journal of Inorganic and Organometallic Polymers and Materials*, **2021,** *31*, 886-897.

[46]. Verma, M.; Mitan, M.; Kim, H.; Vaya, D. Efficient photocatalytic degradation of Malachite green dye using facilely synthesized cobalt oxide nanomaterials using citric acid and oleic acid. *Journal of Physics and Chemistry of Solids*. **2021,** 155, 110125.